JOURNAL OF VIROLOGY, Oct. 2009, p. 9672–9681 Vol. 83, No. 19
0022-538X/09/$08.00+0 doi:10.1128/JVI.00597-09

Molecular Mechanism of BST2/Tetherin Downregulation by K5/MIR2 of Kaposi's Sarcoma-Associated Herpesvirus[▽]

Mandana Mansouri, Kasinath Viswanathan, Janet L. Douglas, Jennie Hines, Jean Gustin, Ashlee V. Moses, and Klaus Früh*

Vaccine and Gene Therapy Institute, Oregon Health and Science University, Beaverton, Oregon

Received 23 March 2009/Accepted 8 July 2009

K3/MIR1 and K5/MIR2 of Kaposi's sarcoma-associated herpesvirus (KSHV) are viral members of the membrane-associated RING-CH (MARCH) ubiquitin ligase family and contribute to viral immune evasion by directing the conjugation of ubiquitin to immunostimulatory transmembrane proteins. In a quantitative proteomic screen for novel host cell proteins downregulated by viral immunomodulators, we previously observed that K5, as well as the human immunodeficiency virus type 1 (HIV-1) immunomodulator VPU, reduced steady-state levels of bone marrow stromal cell antigen 2 (BST2; also called CD317 or tetherin), suggesting that BST2 might be a novel substrate of K5 and VPU. Recent work revealed that in the absence of VPU, HIV-1 virions are tethered to the plasma membrane in BST2-expressing HeLa cells. By targeting BST2, K5 might thus similarly overcome an innate antiviral host defense mechanism. Here we establish that despite its type II transmembrane topology and carboxy-terminal glycosylphosphatidylinositol (GPI) anchor, BST2 represents a bona fide target of K5 that is downregulated during primary infection by and reactivation of KSHV. Upon exit of the protein from the endoplasmic reticulum, lysines in the short amino-terminal domain of BST2 are ubiquitinated by K5, resulting in rapid degradation of BST2. Ubiquitination of BST2 is required for degradation, since BST2 lacking cytosolic lysines was K5 resistant and ubiquitin depletion by proteasome inhibitors restored BST2 surface expression. Thus, BST2 represents the first type II transmembrane protein targeted by K5 and the first example of a protein that is both ubiquitinated and GPI linked. We further demonstrate that KSHV release is decreased in the absence of K5 in a BST2-dependent manner, suggesting that K5 contributes to the evasion of intracellular antiviral defense programs.

Bone marrow stromal cell antigen 2 (BST2) was recently identified as a host cell restriction factor that prevents the release of retroviral and filoviral particles from infected host cells (23). Human immunodeficiency virus type 1 (HIV-1) counteracts this antiviral function of BST2 by expressing the viral auxiliary protein VPU (41, 53). In the absence of VPU, virus particles are prevented from budding off the cellular membrane in cells that express BST2, resulting in virions being tethered to the plasma membrane. BST2 was therefore renamed tetherin (41), although questions still remain as to whether BST2 acts as the actual tether and whether BST2-dependent tethering occurs in all BST2-expressing cell types (36). Independently, BST2 was shown to be induced by type I and type II interferons (IFNs) (7), suggesting that BST2 is part of the innate antiviral response triggered in infected cells.

Using a quantitative membrane proteomic approach, we observed that BST2 is underrepresented in plasma membranes from cells expressing not only VPU (14) but also the K5 protein of Kaposi's sarcoma-associated herpesvirus (KSHV) (4). K5 is a viral homologue of a family of cellular transmembrane ubiquitin ligases, termed membrane-associated RING-CH (MARCH) proteins (3), that mediate the ubiquitination of the cytoplasmic portion of transmembrane proteins (reviewed in reference 40). Each member of this family targets a subset of cellular membrane proteins with both unique and shared specificities (4, 56). One of the functions of cellular MARCH proteins is to modulate antigen presentation by mediating the ubiquitin-dependent turnover of major histocompatibility complex (MHC) class II molecules in dendritic cells, B cells, and monocytes/macrophages (43, 52). In contrast, viral homologues of MARCH proteins encoded by KSHV, murine herpesvirus 68, and the leporipoxvirus myxomavirus all share the ability to mediate the destruction of MHC-I (reviewed in reference 16) but not MHC-II molecules. Thus, one of the functions of the viral proteins is to promote viral escape from immune clearance by $CD8^+$ T lymphocytes (50). Furthermore, each viral MARCH homologue specifically eliminates additional host cell proteins, so each plays multiple roles in viral pathogenesis. KSHV carries two viral MARCH proteins, K3 and K5, also known as MIR1 and MIR2, which both support viral escape from T-cell, NK-cell, and NKT-cell recognition by eliminating the corresponding ligands from the surfaces of infected cells (reviewed in reference 10). In endothelial cells (ECs), K5 additionally downregulates EC-specific adhesion molecules that play an essential role in the formation of adhesive platforms and adherens junctions (31, 32). Since Kaposi's sarcoma is a tumor of EC origin, K5 might thus also contribute to tumorigenesis by disrupting normal EC barrier function and by modulating the interaction of ECs with inflammatory leukocytes.

The downregulation of BST2 by K5 further suggests that K5 also counteracts innate antiviral responses, which might benefit KSHV. However, most transmembrane proteins targeted by viral or cellular MARCH proteins are type I transmembrane

* Corresponding author. Mailing address: Vaccine and Gene Therapy Institute, Oregon Health and Science University, 505 NW 185th Ave., Beaverton, OR 97006. Phone: (503) 418-2735. Fax: (503) 418-2701. E-mail: Fruehk@ohsu.edu.

▽ Published ahead of print on 15 July 2009.

proteins that belong to the immunoglobulin superfamily. In contrast, BST2 is a type II transmembrane protein that is also glycosylphosphatidylinositol (GPI) anchored (25). Thus, BST2 has a short cytoplasmic amino terminus followed by an outside-in transmembrane domain, a large glycosylated extracellular portion, and a GPI anchor. The additional propensity of BST2 to form homodimers (44) was speculated to be crucial for the tethering function of BST2 in that self-association of BST2 molecules in the viral envelope with plasma membrane BST2 could prevent viral exit (19). The unusual topology of BST2 and its multimerization raised the question of whether BST2 is a bona fide target of K5 or whether its downregulation is a downstream effect of K5 eliminating other transmembrane proteins. Additionally, it is not clear whether BST2 would be downregulated in the context of a normal viral infection and, particularly, whether virally expressed K5 would be able to overcome the high expression levels of BST2 observed upon IFN induction. We now demonstrate that KSHV efficiently downregulates IFN-induced BST2 both during primary infection and upon reactivation from latency in ECs. IFN-induced BST2 is ubiquitinated by K5 upon exiting the endoplasmic reticulum (ER) and is rapidly degraded by a pathway that is sensitive to proteasome inhibitors but resistant to inhibitors of lysosomal acidification. These data suggest that despite its unusual topology, BST2 is directly targeted by K5. We further demonstrate that BST2 reduces KSHV release upon inhibition of K5 expression by small interfering RNA (siRNA), suggesting that BST2 is part of the IFN-induced innate immune response to KSHV. Thus, in addition to contributing to viral evasion of cellular immune responses and remodeling EC function, K5 also counteracts the innate immune defense of the host cell.

MATERIALS AND METHODS

Viruses and cell culture. Dermal microvascular endothelial cells (DMVECs) were immortalized by transfection with human papillomavirus (HPV) E6 and E7 and infected with KSHV as described previously (37). KSHV was obtained from reactivated BCBL-1 cells as described previously (37). Replication-deficient adenovirus expressing N-terminally (K3) or C-terminally (K5) FLAG-tagged inserts under the control of a Tet transactivator-dependent promoter and Ad-RTA were described previously (32). Ad-TET was obtained from David Johnson, Oregon Health and Science University.

HeLa cells were infected with rKSHV.219 (kindly provided by J. Vieira). rKSHV.219 expresses green fluorescent protein (GFP) under the control of a constitutive promoter and red fluorescent protein under the control of a lytic promoter and exhibits puromycin resistance (55). Latently infected cells were plated in six-well plates and were treated with control, K5, or BST-2 siRNA, using Lipofectamine 2000 transfection reagent following the manufacturer's protocol. The transfection was repeated after 8 h. Ad-RTA was used to reactivate the virus in latently infected cells. Forty-eight hours after infection, supernatants were collected, filtered, and used to infect 293 cells. Cells were analyzed by flow cytometry after 48 h to measure GFP fluorescence.

To generate stable cell lines expressing BST2, the human *bst-2* cDNA was amplified as an NheI/BamHI fragment by a PCR using the *Pfu* enzyme (Stratagene, San Diego, CA) and inserted into the lentiviral vector pCDH-CMV-MCS-EF1-Puro (System Biosciences, Mountain View, CA). BST2 and its mutants with a hemagglutinin (HA) tag at position 146 (BST2-HA) and lysine-to-arginine replacements at positions 18 and 21 (BST2-KR) were generated by primer-directed mutagenesis using PCR. Lentiviral supernatants were produced via triple transfection of 293T cells with the pHP-dl-N/A packaging construct, the pHEF-VSVG envelope construct (both constructs were obtained through the AIDS Research and Reference Reagent Program, Division of AIDS, NIAID, NIH, from Lung-Ji Chang [9]), and one of the lentiviral clones described above. Transfections were performed using Effectene (Qiagen, Germantown, MD), with a plasmid ratio of 6:1:3 (packaging construct:envelope construct:lentiviral clone). After 48 h, the supernatants were collected and lentiviruses were purified through a 0.8-μm filter. Stable cell lines expressing BST2, BST2-HA, BST2-HA-KR, and BST2-KR were generated by lentiviral transduction and puromycin selection (0.3 μg/ml). An empty pCDH vector was used as a control.

Antibodies and reagents. Mouse anti-human BST2 (HM 1.24) was kindly provided by Chugai Pharmaceutical Co., Ltd. (Kanagawa, Japan), and was previously characterized (44). This antibody was used for cytofluorometry (1:200), immunofluorescence (1:100), immunoprecipitation (1 μg/ml of lysate), and immunoblotting (1:2,000). Anti-ubiquitin (clone P4D1) and anti-glyceraldehyde-3-phosphate dehydrogenase (anti-GAPDH) were obtained from Santa Cruz Biotechnology (Santa Cruz, CA). Mouse anti-human HLA antibody W6/32 was obtained from Sigma (St. Louis, MO), and anti-HA antibody was obtained from Covance Research Products Inc. (Denvar, PA). Anti-K5 antibody was described previously (45).

The following reagents were used at the indicated concentrations. Concanamycin A (ConA) (working concentration, 50 nM) was purchased from Sigma (St. Louis, MO). MG132 was obtained from Boston Biochem (Cambridge, MA) and used at a final concentration of 20 μM. Human β-IFN (PBL Biomedical Laboratories, Piscataway, NJ) was used at 500 U/ml, and recombinant human tumor necrosis factor alpha (TNF-α; R&D Systems, Minneapolis, MN) was used at 10 ng/ml. Dominant-negative VPS4 (GFP-E228Q) and wild-type GFP-VPS4 plasmids were obtained from Wes Sundquist (18).

Cell surface protein biotinylation. Cell surface proteins were biotinylated with EZ-Link NHS-SS-biotin following the manufacturer's protocol (Pierce, Rockford, IL). Briefly, cells were washed three times with ice-cold phosphate-buffered saline (PBS), and primary amines of the membrane proteins exposed to the exterior of the cells were biotinylated with NHS-SS-biotin for 30 min at 4°C. The cells were washed and lysed immediately with a nonionic detergent. Labeled proteins were isolated with immobilized NeutrAvidin (Pierce, Rockford, IL). The bound proteins were released by incubating the resin with sodium dodecyl sulfate-polyacrylamide gel electrophoresis (SDS-PAGE) sample buffer containing 50 mM dithiothreitol.

Metabolic labeling and immunoprecipitation. Cells were starved in Dulbecco's modified Eagle's medium deficient in methionine and cysteine for 30 min and then pulse labeled for 15 min with 80 μCi/ml L-[^{35}S]methionine and 24 μCi/ml L-[^{35}S]cysteine (Express protein labeling mix; PerkinElmer, Boston, MA). The label was chased for various times with full medium containing an excess of normal cysteine and methionine. Cells were lysed in SDS buffer (1% NP-40), and antigens were immunoprecipitated with 1 μg/ml of antibody. Precipitates were either left untreated or treated with 1 μg of endo-β-*N*-acetylglucosaminidase H (endo H) or 500 U of *N*-glycosidase F (PNGase F; New England Biolabs, Ipswich, MA). The proteins were separated in a 10% SDS gel, dried, and exposed to Kodak Biomax MR film. Treatment with MG132 (20 μM) or ConA (50 nM) was done for 12 h after transduction with Ad-K5 for 4 h.

Immunoblotting of immunoprecipitated BST2. To solubilize BST2, 6×10^5 cells were lysed in 250 μl of 0.6% SDS in PBS at room temperature for 20 min and then scraped off and diluted, using 750 μl of 1.2% Triton X-100. The cell lysate was cleared of debris by centrifugation at 10,000 × *g* for 10 min at 4°C. BST2 was immunoprecipitated using 1 μg of HM1.24 antibody. The immunoprecipitate was washed in 0.2% Triton X-100, resuspended in gel loading buffer (10% glycerol, 5% β-mercaptoethanol, 2% SDS, 50 μM Tris, pH 6.8, and 0.02% bromophenol blue), and separated by 10% SDS-PAGE. The proteins were transferred to a polyvinylidene difluoride membrane (Waters Ltd., Milford, MA) and probed with primary antibodies for 1 h at room temperature, followed by horseradish peroxidase-conjugated secondary antibody (Santa Cruz Antibody Solutions). Membranes were washed in 0.1% Tween 20 in PBS. The proteins were detected using a SuperSignal West Femto chemiluminescence kit (Thermo Scientific, Rockford, IL).

qPCR. Total mRNA from cells was isolated and purified using RNeasy (Qiagen). Specific primers for BST2, K5, and β-actin were designed using Primer 3 software (BST2 primers were CCGTCCTGCTCGGCTTT [forward] and CC GCTCAGAACTGATGAGATCA [reverse], K5 primers were ACAAGGACC GTCAATTCGATG [forward] and TGCCATACCGACGGCC [reverse], and β-actin primers were TCACCCACACTGTGCCCATCTACGA [forward] and CAGCGGAACCGCTCATTGCCAATGG [reverse]). Transcript levels were determined by quantitative real-time reverse transcriptase PCR (qPCR), using SYBR green dye incorporation (AB Applied Biosystems, Warrington, United Kingdom) and AmpliTaq Gold DNA polymerase in an ABI Prism 7900HT sequence detection system (AB Applied Biosystems, Warrington, United Kingdom). The comparative threshold cycle method was used to derive the change in BST2 expression between different treatments, using β-actin as an internal standard (46).

RESULTS

KSHV downregulates IFN-induced BST2 during primary infection. Using quantitative proteomics, we previously observed that BST2 was underrepresented in membrane preparations of K5-expressing HeLa cells (4). The mass spectrometric result was independently verified using a commercially available anti-BST2 antiserum that was of limited specificity and could be used only in immunoblots. To independently verify that BST2 is downregulated by K5 in a cell type that can be infected with KSHV, we studied BST2 expression in HPV E6/E7-immortalized DMVECs (E-DMVECs) (37), using the BST2-specific monoclonal antibody HM1.24 (kindly provided by Chugai Pharmaceuticals) (44). In untreated DMVECs, we observed low levels of BST2 expression at the cell surface (Fig. 1A). However, a significant increase in the BST2 surface level occurred upon treatment with IFN-β, consistent with previous reports that BST2 is inducible by IFN (7). A similar induction was observed upon treatment with TNF-α (Fig. 1A). In contrast, prior transduction of DMVECs with an adenovirus expressing K5 (Ad-K5) reduced IFN-β-induced BST2 expression, whereas transduction with Ad-K3 or Ad-TET alone had no effect on IFN induction of BST2 (Fig. 1B). These data confirm our previous observations with HeLa cells, which express BST2 constitutively, and demonstrate that K5 is able to downregulate BST2 expression upon IFN induction in cells representative of Kaposi's sarcoma.

Upon de novo infection of E-DMVECs, KSHV establishes latent infection (37). Prior to establishment of latency, however, K5 is transiently expressed (24), although protein levels in the majority of cells are typically below the limits of detection by standard methods (1). Upon primary infection of DMVECs with KSHV, a significant reduction of BST2 surface expression was observed in IFN-induced DMVECs (Fig. 1B). The percentage of cells expressing low levels of BST2 corresponded to cells that were LANA-1 positive (not shown). To determine whether BST2 downregulation was the consequence of transient K5 expression in primary infected DMVECs, we pretreated DMVECs with siRNA to K5 or control siRNA, as described previously (1, 32), prior to KSHV infection. As shown in Fig. 1B, BST2 was downregulated in control siRNA-treated cells, but KSHV had no effect on BST2 levels upon treatment with K5 siRNA. Reduction of K5 protein expression by siRNA was verified by immunoblotting (Fig. 1C). Taken together, these data suggest that during de novo infection, KSHV downregulates BST2 by expressing K5.

KSHV inhibits IFN-induced BST2 expression upon reactivation from latency. To examine whether KSHV is able to prevent IFN-induced BST2 upregulation during latency or upon reactivation from latency, we studied BST2 expression in latently infected or reactivated E-DMVECs. Latently infected E-DMVECs were generated as described previously (37). As shown in Fig. 2A, latently infected cells did not counteract IFN-induced BST2 upregulation, consistent with a lack of K5 expression during established latency. Latent virus can be reactivated experimentally by introduction of the viral transactivator RTA, which induces lytic genes, including the K5 gene (51). Upon reactivation of KSHV by transduction of latently infected cells with Ad-RTA, we observed a significant inhibition of IFN-induced BST2 surface expression, whereas Ad-TET was unable to prevent BST2 induction (Fig. 2A). This correlated with the strong induction of K5 expression (Fig. 2B). Since KSHV carries several modulators of IFN signaling (42), it was possible that reactivated KSHV prevented BST2

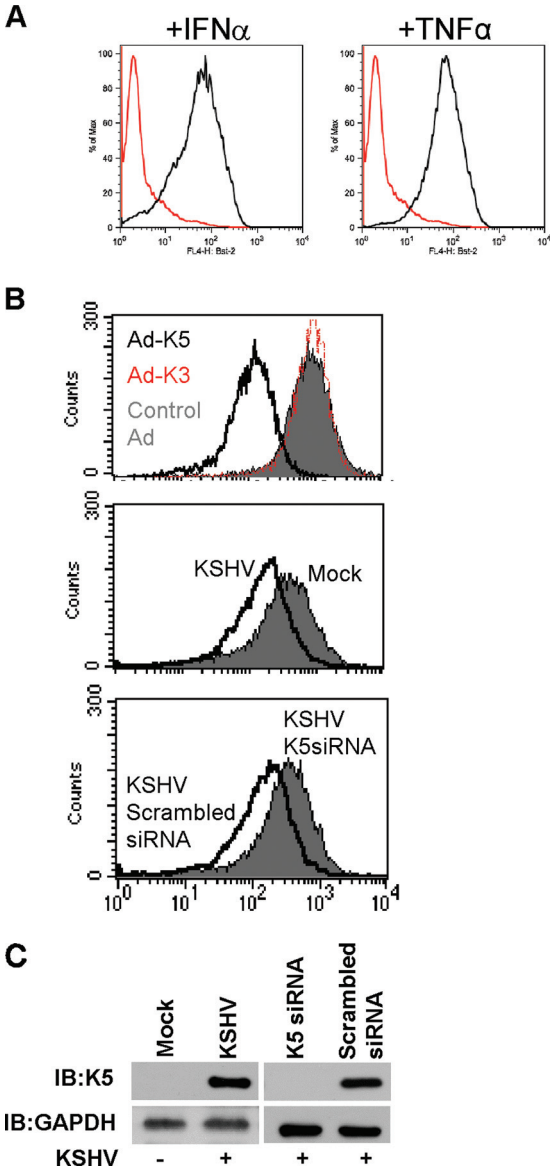

FIG. 1. K5 downregulates IFN-induced BST2 in DMVECs infected with KSHV. (A) BST2 is induced by IFN-β and TNF-α in DMVECs. E-DMVECs were treated with 500 U/ml of human IFN-β or 10 ng/ml TNF-α for 24 h or were left untreated (red) prior to flow cytometry with anti-BST2 (HM1.24). (B) K5 downregulates IFN-β-induced BST2 during de novo infection with KSHV. (Top) E-DMVECs were transduced with Ad-K5 (black), Ad-K3 (red), or Ad-TET (gray) for 24 h prior to treatment with IFN-β and flow cytometry for BST2. (Middle) E-DMVECs were infected with KSHV (white) or mock infected (gray) prior to treatment with IFN-β and staining for BST2. (Bottom) E-DMVECs were treated with K5-specific (white) or scrambled (gray) siRNA and infected with KSHV prior to treatment with IFN-β and staining for BST2. (C) K5-specific siRNA inhibits K5 protein expression during primary infection. Duplicate samples from the middle and lower parts of panel B were used to confirm K5 knockdown by K5 siRNA. Cells were lysed and immunoblotted with anti-K5 or anti-GAPDH antibody.

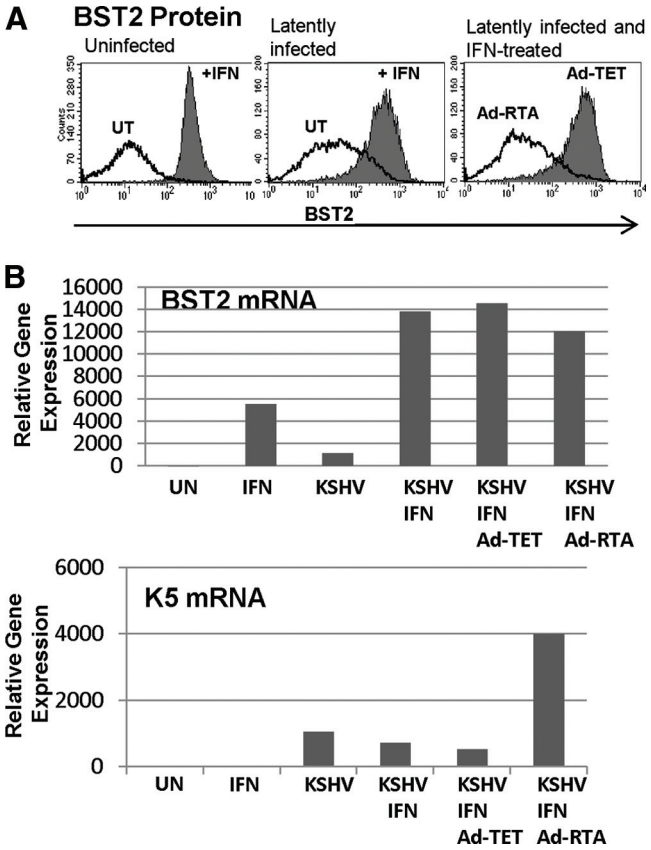

FIG. 2. KSHV inhibits induction of BST2 protein, but not mRNA, upon reactivation. (A) BST2 downregulation upon viral reactivation. (Left) Uninfected E-DMVECs were treated with IFN-β for 24 h (+IFN; gray) or were left untreated (UT; black) prior to being stained with anti-BST2 (HM1.24). (Middle) E-DMVECs latently infected with KSHV were treated with IFN-β (+IFN; gray) or left untreated (UT; black). (Right) Latently infected E-DMVECs were transduced with Ad-RTA (black) or Ad-TET (gray) prior to treatment with IFN-β for 24 h. (B) KSHV does not inhibit induction of BST2 mRNA by IFN-β. BST2 (top) and K5 (bottom) mRNA levels were quantified by qPCR for cells treated as described for panel A. Results were normalized to a β-actin control, and changes compared to untreated, uninfected E-DMVECs were calculated using the comparative threshold cycle method as described previously (46).

induction at the transcriptional level. However, qPCR of BST2-specific transcripts revealed a strong induction of a BST2-specific message upon IFN induction in both latently infected and reactivated samples (Fig. 2B). Therefore, we concluded that during reactivation, BST2 expression is inhibited at a posttranscriptional level, consistent with K5-mediated degradation. In contrast to the case with primary infected cells, however, we did not observe increased BST2 expression upon treatment of reactivated cells with K5-specific siRNA due to incomplete gene knockdown (data not shown). Since very low levels of K5 are sufficient to downregulate target proteins (1), presumably due to the catalytic nature of ubiquitin ligases, the efficient reactivation of K5 expression by Ad-RTA seems to outcompete the K5-specific siRNA. However, the fact that BST2 expression is inhibited at a posttranscriptional level strongly suggests that K5 is responsible for this effect upon viral reactivation from latency.

BST2 is degraded upon exiting the ER. BST2 is an unusual transmembrane protein that has a type II transmembrane topology while also carrying a carboxy-terminal GPI anchor. As such, it is very different from all other transmembrane proteins that are targeted by K5, i.e., type I transmembrane proteins belonging to the immunoglobulin superfamily. To determine how BST2 is downregulated by KSHV K5, we studied the fate of BST2 in the presence of K5. The effects of K5 on cell surface-expressed and total BST2 were monitored by cell surface biotinylation and immunoblotting of total cell lysates, respectively. In IFN-induced DMVECs transduced with Ad-TET, cell surface biotinylated BST2 appeared as several protein bands that corresponded in molecular size to monomeric (36 kDa), dimeric (>64 kDa), and multimeric forms of BST2, as described previously (44) (Fig. 3A). In the presence of K5, all forms of BST2 were undetectable, suggesting that K5 efficiently prevented surface expression of IFN-induced BST2. A similarly strong reduction was observed for total levels of BST2 by immunoblotting of total SDS lysates (Fig. 3B), suggesting that IFN-induced BST2 was efficiently eliminated by K5.

To facilitate the study of the K5-mediated degradation of BST2 by use of a commercially available antibody, we generated human fibroblasts stably expressing wild-type BST2 or modified BST2 containing an internal HA epitope tag at a nonconserved site (41). BST2-HA was initially synthesized as an endo H-sensitive protein of approximately 24 kDa that was converted into an endo H-resistant form of approximately 36 kDa (Fig. 3C). Upon PNGase F treatment, the 36-kDa protein was converted to the same low molecular mass as the endo H-sensitive form. Since the predicted molecular mass of BST2 is 19.6 kDa, we concluded that the low-molecular-mass form corresponded to deglycosylated BST2. The large shift in molecular mass is consistent with both predicted glycosylation sites being used (44). The 36-kDa mature protein is relatively long-lived, with a half-life of more than 6 h. In the presence of K5, the synthesis of the endo H-sensitive form of BST2 was unhampered. However, the endo H-resistant form of BST2 was short-lived, with a half-life of less than 2 h. Since endo H resistance indicates that BST2 has acquired modified N-linked glycans in the Golgi apparatus, these results indicate that K5 mediates the degradation of BST2 in a post-ER compartment. Since we were unable to detect BST2 at the cell surface by biotinylation, it further seems that K5 intercepts BST2 en route to the cell surface.

Proteasome inhibitors, but not endosomal inhibitors, prevent BST2 degradation. Post-ER degradation implies that BST2 is targeted for degradation in lysosomes via the multivesicular body (MVB) pathway, as described for several other K5 targets (26). In such instances, K5-mediated degradation could be inhibited using small-molecule inhibitors of vacuolar ATPases, such as the macrolide ConA (30–32). Surprisingly, however, surface expression of BST2 was not restored in the presence of ConA (Fig. 4A). In contrast, the proteasome inhibitor MG132 completely restored BST2 surface expression (Fig. 4A). To determine whether proteasomal or endo/lysosomal inhibitors prolonged the half-life of BST2, we performed pulse-chase experiments, with MHC-I molecules as a control. As shown in Fig. 4B, MG132 efficiently prevented the degradation of both MHC-I molecules and BST2. In contrast, ConA prolonged the half-life of BST2 but ultimately did not prevent

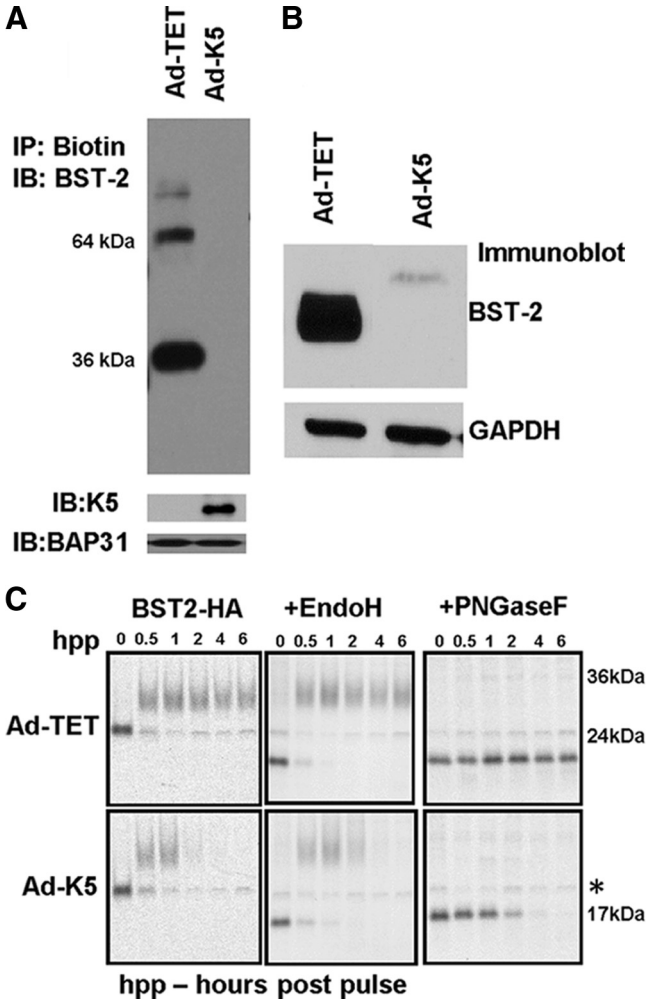

FIG. 3. Degradation of BST2 by K5. (A) BST2 is absent from the cell surface in the presence of K5. E-DMVECs were transduced with Ad-K5 or Ad-TET alone for 24 h, followed by treatment with 500 U/ml IFN-β. After 24 h, cell surface-expressed proteins were biotinylated. Upon cell lysis, biotinylated proteins were captured with avidin and separated by SDS-PAGE. BST2 was visualized by immunoblotting with anti-BST2 (top), anti-K5 (middle), or anti-BAP31 (bottom) as a loading control. (B) K5 reduces steady-state levels of BST2. E-DMVECs were transduced with Ad and treated with IFN-β as described for panel A. Cells were lysed in SDS sample buffer, and the lysate was separated by SDS-PAGE followed by immunoblotting with HM1.24 or anti-GAPDH. (C) Increased degradation of endo H-resistant BST2 by K5. Human fibroblasts stably transfected with the lentivector pCDH-BST2-HA were pulse labeled for 15 min, followed by a chase, as indicated. BST was immunoprecipitated with anti-HA after treatment, followed by treatment with endo H or PNGase F when indicated. SDS-PAGE and autoradiography revealed a 24-kDa glycosylated endo H-sensitive precursor that was converted to an ~34-kDa endo H-resistant glycoprotein. Deglycosylated BST2 migrated at about 17 kDa, consistent with its predicted molecular mass of 19 kDa. A nonspecific 24-kDa band comigrated with the 24-kDa form of BST2 (*).

its degradation, whereas MHC-I degradation was completely inhibited. This result was unexpected since the proteasome is unable to degrade transmembrane proteins once they have exited the ER. An alternative explanation for this result is that MG132 treatment is known to deplete free ubiquitin from cells, thus affecting ubiquitin-mediated endocytosis (33). Moreover, proteasome inhibitors were previously shown to prevent sorting of MHC-I to late endosomal complexes of K3-expressing cells (28). To determine whether BST2 was targeted to lysosomes via the MVB pathway, we cotransfected K5, K3, or a control plasmid with VPS4 or the EQ mutant of VPS4, which inhibits MVB formation (18). BST2 surface levels, monitored by flow cytometry, were reduced in the presence of VPS4, but to a much lesser extent in the presence of VPS4-EQ (Fig. 4C). Therefore, we concluded that K5 targets BST2 for lysosomal destruction via the MVB pathway. Why endo/lysosomal targeting of BST2 by K5 was less sensitive to proton pump inhibitors than MHC-I targeting remains to be investigated.

Ubiquitination of cytoplasmic lysines is required for BST2 downregulation. As a ubiquitin ligase, K5 transfers ubiquitin to the cytoplasmic (and usually carboxy-terminal) portion of its substrates (12). Ubiquitin is conjugated to lysines but can also be transferred to cysteines in the absence of lysines (8). To determine whether BST2 is ubiquitinated in the presence of K5 and whether this ubiquitination is necessary for BST2 downregulation, we replaced two amino-terminal lysines that are predicted to face the cytosol (K18 and K21) with arginines. The resulting construct, BST2-KR, as well as wild-type BST2, was stably transfected into human fibroblasts. When transfectants were transduced with Ad-K5, only BST2 was significantly downregulated (Fig. 5A). In contrast, BST2-KR was largely unaffected. In human fibroblasts stably transfected with an HA-tagged version of BST2-KR, the half-life of BST2 in the presence of K5 was nearly indistinguishable from that in Ad-TET-transduced cells. In contrast, MHC-I molecules immunoprecipitated from the same lysates were turned over more rapidly in Ad-K5- than in Ad-TET-transduced cells. These observations strongly suggested that ubiquitination plays an essential role in BST2 downregulation by KSHV K5. To further determine whether the cytosolic lysines were ubiquitinated in the presence of K5, we immunoprecipitated BST2-HA or BST2-KR-HA from Ad-K5- or Ad-TET-transduced stably transfected fibroblasts and probed immunoblots with ubiquitin-specific antibodies. As shown in Fig. 5C, several high-molecular-weight bands appeared in immunoblots for Ad-K5-transduced fibroblasts. These ubiquitin-reactive bands were absent for Ad-TET- or Ad-K5-transduced BST2-KR-HA-expressing cells. We concluded that they represent oligo-ubiquitinated BST2 and that ubiquitination takes place at the intracellular lysines. Interestingly, a low-molecular-weight ubiquitinated protein was immunoprecipitated with BST2-KR-HA in the presence of K5. The identity of this protein is currently unknown, but it might represent a protein that is ubiquitinated in a complex with K5 and BST-KR. We further examined the effect of MG132 on BST2 ubiquitination. As shown in Fig. 5C, ubiquitinated BST2 was not detected in the presence of MG132, consistent with MG132 inhibiting ubiquitination of BST2. In contrast, ConA did not affect ubiquitination of BST2 and did not stabilize a ubiquitinated intermediate as observed previously (31, 32). We therefore concluded that MG132 restored BST2 surface expression by depleting free ubiquitin and thus preventing K5 from ubiquitinating BST2.

BST2 reduces KSHV recovery. To determine whether BST2 affects the production of KSHV upon reactivation, we infected HeLa cells, which express high levels of endogenous BST2 (4), with rKSHV.219, a recombinant virus that expresses GFP un-

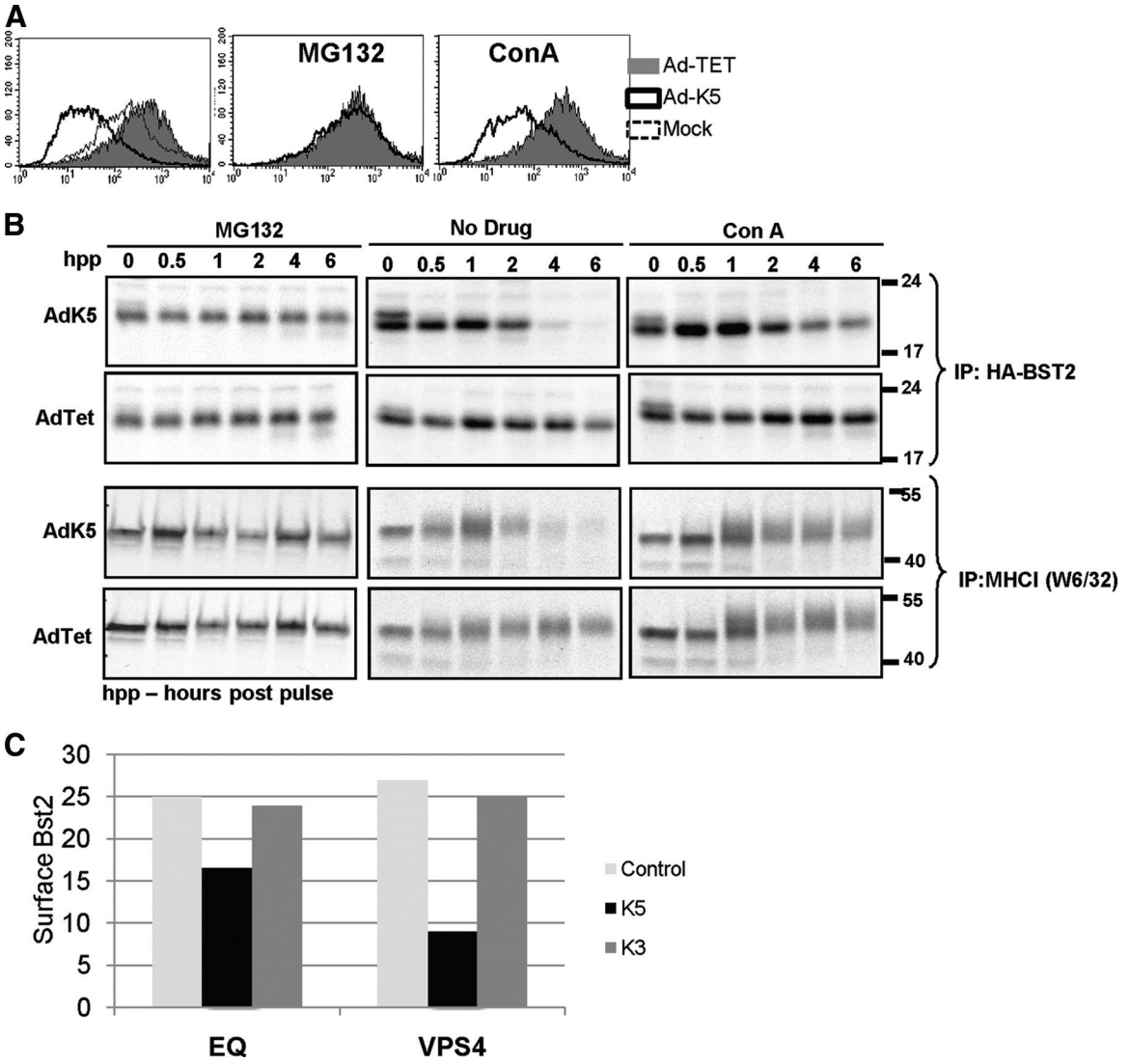

FIG. 4. Proteasomal but not lysosomal inhibitors prevent K5-mediated BST2 degradation. (A) Proteasome inhibitors restore cell surface expression of BST2 in the presence of K5. Stable transfectants expressing BST2-HA were mock treated (dashed line) or transduced with Ad-K5 (black line) or Ad-TET (gray area) for 24 h, followed by treatment with MG132 (20 μM) or ConA (50 nM) for 12 h. BST2 expression was monitored by flow cytometry using anti-HA. (B) Proteasome inhibitors prevent K5-mediated BST2 degradation. Human fibroblasts stably expressing BST2-HA were metabolically labeled for 15 min, and the label was chased for the indicated times prior to immunoprecipitation and PNGase F treatment. Prior to being labeled, human fibroblasts were pretreated for 12 h with MG132 (20 μM) or left untreated. Immunoprecipitation was done with anti-HA antibody. (C) Overexpression of dominant-negative VPS4-EQ partially restores BST2 surface expression compared to wild-type VPS4 in K5-transfected cells. HeLa cells were cotransfected with control plasmid, K5, or K3 and with wild-type VPS4 or VPS4-EQ. Twenty-four hours later, transfected cells were analyzed by flow cytometry. Surface expression of BST2 on VPS4-expressing cells (as detected by GFP positivity) was measured by flow cytometry using anti-BST2.

der the control of a constitutive promoter and red fluorescent protein under the control of a lytic promoter (55). rKSHV.219 established latent infection in HeLa cells upon puromycin selection, as described previously (55). Latently infected cells were treated with siRNA to K5 or control siRNA, and virus was reactivated with Ad-RTA together with sodium butyrate. Virus release into the supernatant was monitored by transferring the supernatant to HEK293 cells and monitoring GFP fluorescence. As shown in Fig. 6A, we observed a 50% reduction of KSHV recovery from HeLa cells in the presence of K5 siRNA. This reduction of KSHV release was due to BST2, since KSHV recovery was restored to control levels when K5 siRNA was cotransfected with siRNA to BST2 prior to reactivation (Fig. 6B). Cotransfection of the two siRNAs did not affect their ability to reduce target transcript expression (Fig. 6C). We interpret these results as an indication that BST2 interferes with KSHV release.

DISCUSSION

Our data strongly suggest that despite its unusual topology, BST2 is a bona fide target of K5. As such, K5 mediates the ubiquitination of one or both cytoplasmic lysines at a post-ER location in the cell. Previously, it was demonstrated that BST2

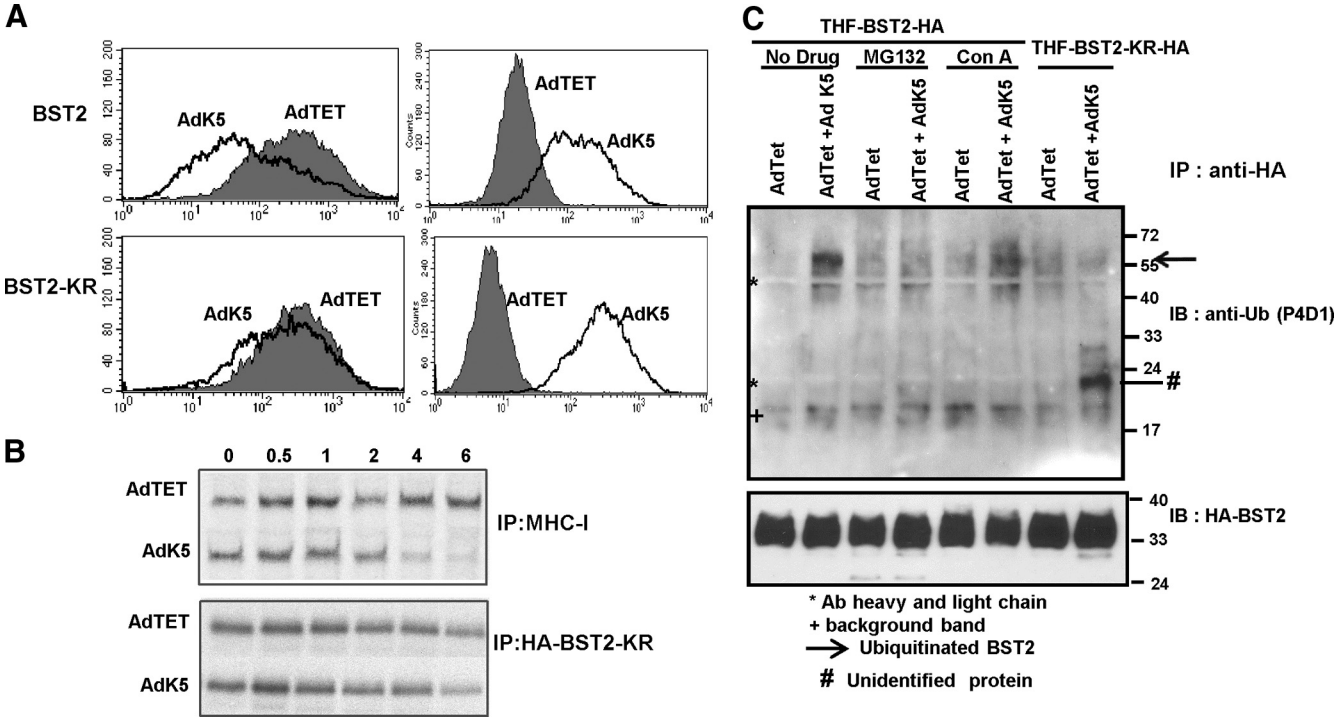

FIG. 5. Ubiquitination of cytoplasmic lysines of BST2 is required for K5-mediated degradation. (A) Cytoplasmic lysines are required for BST2 downregulation from the cell surface. Flow cytometry was performed with human fibroblasts stably transfected with BST2 or lysine-deleted BST2-KR and transduced with Ad-K5 (black) or Ad-TET (gray) for 24 h. BST2 was detected with the anti-BST2 antibody. (B) Lysine-deleted BST2 is resistant to K5-mediated degradation. BST2-KR-HA-expressing fibroblasts were transduced with Ad-K5 or Ad-TET for 24 h, followed by pulse-chase metabolic labeling and immunoprecipitation with antibodies to MHC-I (W6/32) or anti-HA. Note that the half-life of MHC-I molecules was decreased in the presence of K5, whereas that of BST2-KR-HA was unaffected. (C) BST2 is ubiquitinated in the presence of K5. BST2-HA-expressing fibroblast cells were transduced with Ad-TET alone or with Ad-TET and Ad-K5 in the presence of MG132, ConA, or no drug for 10 h. The cells were harvested, immunoprecipitated using anti-HA antibody, and immunoblotted with anti-ubiquitin antibody (P4D1). Likewise, BST2-KR-HA-expressing fibroblasts were transduced with Ad-TET alone or with Ad-TET and Ad-K5 for 10 h and then immunoprecipitated and immunoblotted. Nonspecific and unidentified protein bands are indicated. Ab, antibody.

continuously recycles between the plasma membrane and the *trans*-Golgi network (TGN) (25). In contrast to other K5 targets that are internalized from the cell surface (11, 31), we were unable to detect BST2 at the plasma membrane, even upon biotinylation (Fig. 3A). Thus, K5 most likely intercepts IFN-induced BST2 in the TGN. This conclusion is also supported by the observation that K5 does not degrade BST2 prior to ER exit.

Given the post-ER degradation of BST2, the most likely destination of ubiquitinated BST2 is the lysosome. Surprisingly, however, inhibitors of lysosomal acidification did not prevent K5-mediated BST2 degradation. This is in contrast to the case for all other K5 targets (with the notable exception of newly synthesized CD31 [31]) studied to date (reviewed in reference 40). In each case tested, vacuolar ATPase inhibitors restored surface expression of the respective K5 targets. Moreover, in several instances we observed that ConA stabilized a ubiquitinated intermediate in the presence of K5 or other viral MARCH proteins (30–32). The failure of ConA to prevent K5-mediated BST2 degradation could thus be interpreted as evidence that BST2 is not degraded by the lysosome. Indeed, inhibitors of the proteasome, the second major proteolytic system in the cell, prevented BST2 degradation and restored BST2 surface expression. However, we consider it unlikely that the proteasome is directly involved in degrading BST2 for several reasons, as follows. (i) Proteasomal degradation of transmembrane proteins requires their retrograde translocation to the cytosol (39), a process that is confined to ER-localized transmembrane proteins. Since BST2 acquired endo H resistance prior to K5-mediated turnover, proteasomal degradation would thus require retrograde transport of BST2 to the ER, for which there is currently no evidence. (ii) We did not observe a degradation intermediate of BST2 in the presence of proteasome inhibitors. In contrast, cytosolic, deglycosylated, and ubiquitinated intermediates have been reported for MHC-I molecules degraded by the proteasome in the presence of human cytomegalovirus US2 and US11 (29). (iii) Proteasomal degradation generally requires polyubiquitination via a lysine 48 linkage (13). In contrast, we observed only a few discreet ubiquitinated bands for BST2, consistent with a model of oligo-ubiquitination via lysine 63 linkage proposed for K3 (15). Mono-ubiquitination at single or multiple cytoplasmic lysine residues as well as K63-linked oligo-ubiquitination has been implicated in endocytosis of proteins destined for lysosomal degradation via the MVB pathway (2, 21, 38, 48). (iv) Inhibition of MVB formation by a dominant-negative form of VPS4 restored BST2 surface expression. Taking all these observations together, we therefore consider it unlikely that

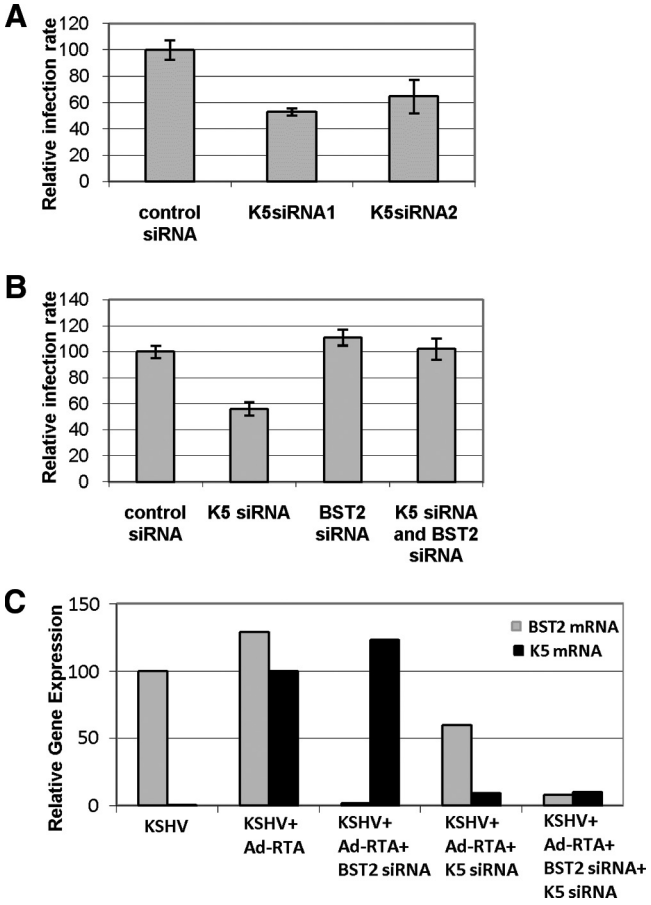

FIG. 6. KSHV K5 facilitates viral release by removing BST2 from HeLa cell surface. (A) Decreased viral release in the presence of K5 siRNA. HeLa cells infected with rKSHV.219 were transfected in triplicate with two K5 siRNAs or control siRNA. The transfections were repeated in 8 h, and 24 h thereafter, Ad-RTA was added to reactivate the virus. After an additional 48 h, cell supernatants were harvested, filtered, and used to infect 293 cells. Forty-eight hours later, GFP fluorescence was monitored in 293 cells by flow cytometry. (B) BST2 siRNA restores KSHV release in the absence of K5. HeLa cells infected with KSHV were transfected with the indicated siRNAs as described for panel A. (C) BST2 and K5 transcript levels upon siRNA treatment. qPCR analysis was performed to determine the relative amounts of BST2 and K5 transcripts in siRNA-transfected HeLa cells infected with KSHV. The K5 transcript level in Ad-RTA-induced KSHV-infected HeLa cells was set to 100%, whereas the BST2 level was set to 100% in the nonactivated KSHV-infected HeLa cells.

BST2 is extracted to the cytosol and destroyed by the proteasome.

A more likely explanation is that MG132 limits the ability of K5 to ubiquitinate BST2, since prolonged treatment with proteasome inhibitors depletes the cellular pool of free ubiquitin (35). This is supported by the observation that ubiquitinated BST2 was no longer observed in MG132-treated cells, despite the presence of K5. Thus, the very first step of ubiquitin-mediated mistargeting of BST2 was inhibited by MG132. Similarly, it was previously concluded that proteasome inhibitors prevent early-to-late endosomal sorting of MHC-I molecules in the presence of KSHV K3 (28). It is thus conceivable that ubiquitin depletion prevents the first step in TGN-to-lysosome mistargeting of BST2. Why this process is resistant to macrolides, such as ConA, that normally block the transport of cargo from late endosomes to lysosomes (54) remains to be investigated.

It is possible that the unique topology and GPI linkage of BST2 contribute to this unusual degradation pathway. The addition of a GPI linker generally renders proteins resistant to ubiquitination due to the concomitant removal of cytoplasmic domains that can be targeted for ubiquitination. To our knowledge, BST2 is the first reported case of a GPI-linked protein that also carries a cytoplasmic domain that is susceptible to ubiquitination. Similar to most GPI-linked proteins localized to cholesterol-rich membrane microdomains, BST2 was shown to localize to lipid rafts (25). Given its unique topology, it was hypothesized that BST2 lines the borders of lipid rafts like a fence, with the N terminus located in the nonraft portion of the membrane. It will be interesting to determine how K5-mediated ubiquitination affects the partitioning of BST2 to lipid rafts and whether other proteins that colocalize with BST2 at lipid rafts are affected by BST2 ubiquitination. For example, ubiquitination could result in the extraction of BST2 from the raft, or it could trigger the mistargeting of other raft-associated proteins. Thus, BST2 ubiquitination by K5 is a unique model with which to study the ubiquitin-mediated sorting of a raft-associated protein.

BST2 downregulation correlated with K5 expression in KSHV-infected ECs. Upon primary infection, K5 is transiently expressed prior to the establishment of a restricted latency-associated expression pattern. Consistent with K5 shutoff during latency, BST2 induction by IFN was not inhibited by K5 in latently infected cells. Instead, basal levels of BST2 were elevated in latently infected cells (Fig. 2), suggesting a low-level activation of BST2 expression in virally infected cells. Given that multiple stimuli (type I and type II IFNs, as well as TNF-α) induce BST2 expression, we interpret this as evidence that infection by KSHV upregulates the transcription of BST2. This IFN-independent, virus-dependent BST2 induction could be due to activation of NF-κB by the latency-associated transcript vFLIP (20). In fact, it was recently reported that human umbilical ECs transduced with vFLIP showed a severalfold upregulation of the BST2 transcript (47). Alternatively, viral DNA could activate innate pattern recognition receptors, such as the recently identified IFN-activating repeat element in γ2-herpesvirus genomes (49). In vivo, BST2 induction might thus result from local IFN secretion by neighboring infected cells or infiltrating lymphocytes as well as from activation of the innate immune response in infected cells.

The targeted elimination of BST2 by K5 is thus part of KSHV's countermeasures against the host IFN response. Several gene products of KSHV are known to interfere at different steps of the IFN cascade, including (i) the signaling pathways that lead to the induction of the IFN gene, (ii) the signaling cascade triggered by IFN binding to its cellular receptors, and (iii) counteraction of the antiviral activity of IFN-stimulated genes (ISGs). For example, viral IFN regulatory factors (vIRFs) disrupt the IFN-independent activation of host IRFs (42). Moreover, IFN-γ-dependent signaling can be counteracted by K3 and K5, which both downregulate the IFN-γ receptor (27), and type I IFN-dependent signal transduction was shown to be inhibited by vIRF2 (17) and by the RIF protein

encoded by ORF10 (6). However, we observed only a slight reduction of BST2 mRNA induction by IFN-β in Ad-RTA-transduced versus control-transduced cells (Fig. 2B), suggesting that any inhibition of signal transduction from the type I IFN receptor by reactivated KSHV was unable to substantially interfere with BST2 induction. The downregulation of BST2 by K5 thus belongs in the category of viral gene products preventing the antiviral action of ISGs. While counteracting ISG function has been described for other viruses (5), very little is known about such ISG countermeasures by KSHV. One example is the inhibition of IRF7, an IFN-induced transcription factor, by ORF45 and vIRF3 (22, 57). Thus, the K5-mediated degradation of BST2 is one of the first examples of KSHV directly destroying an IFN-induced protein.

The efficient inhibition of IFN-induced BST2 expression by K5 implies that K5 might play a role in counteracting an innate immune mechanism. One possibility is that in the absence of K5, BST2 prevents the release of KSHV from the host cell, similar to the case reported for VPU-deleted HIV-1. This hypothesis is supported by our observation that KSHV release from HeLa cells was decreased in the presence of K5 siRNA but restored when BST2 expression was also inhibited. Herpesviral egress is quite different from that of retroviruses and filoviruses, as it involves the envelopment of tegument-covered viral capsids in the TGN followed by exocytosis of virion particles by vesicular transport (34). Thus, it seems likely that BST2 interferes with this process in the TGN. Recent observations further suggest that BST2 inhibition of HIV-1 is confined to certain cell types, e.g., macrophages and HeLa cells, but is less efficient in other cell types, e.g., T cells (36). Since experiments with K5 siRNA in other cell types have so far been inconclusive (data not shown), it is possible that an antiviral activity of BST2 is cell type specific. Since KSHV is capable of infecting a number of cell types, with B cells and ECs being the cells most commonly infected in vivo, further work will be required to determine the effect of BST2 on KSHV propagation in the absence of K5.

ACKNOWLEDGMENTS

This work was funded by NIH grant R01 CA/AI 094011 to K.F.

We gratefully acknowledge the gift of anti-HM1.24 antibody from Chugai Pharmaceuticals. We thank Jeff Vieira, University of Washington, for providing KSHV.219 and Wes Sundquist for VPS4 constructs.

REFERENCES

1. **Adang, L. A., C. Tomescu, W. K. Law, and D. H. Kedes.** 2007. Intracellular Kaposi's sarcoma-associated herpesvirus load determines early loss of immune synapse components. J. Virol. **81:**5079–5090.
2. **Barriere, H., C. Nemes, K. Du, and G. L. Lukacs.** 2007. Plasticity of polyubiquitin recognition as lysosomal targeting signals by the endosomal sorting machinery. Mol. Biol. Cell **18:**3952–3965.
3. **Bartee, E., M. Mansouri, B. T. Hovey Nerenberg, K. Gouveia, and K. Früh.** 2004. Downregulation of major histocompatibility complex class I by human ubiquitin ligases related to viral immune evasion proteins. J. Virol. **78:**1109–1120.
4. **Bartee, E., A. McCormack, and K. Früh.** 2006. Quantitative membrane proteomics reveals new cellular targets of viral immune modulators. PLoS Pathog. **2:**e107.
5. **Basler, C. F., and A. Garcia-Sastre.** 2002. Viruses and the type I interferon antiviral system: induction and evasion. Int. Rev. Immunol. **21:**305–337.
6. **Bisson, S. A., A. L. Page, and D. Ganem.** 2009. A KSHV protein that forms inhibitory complexes with type I interferon receptor subunits, Jak and STAT proteins and blocks interferon-mediated signal transduction. J. Virol. **83:**5056–5066.
7. **Blasius, A. L., E. Giurisato, M. Cella, R. D. Schreiber, A. S. Shaw, and M. Colonna.** 2006. Bone marrow stromal cell antigen 2 is a specific marker of type I IFN-producing cells in the naive mouse, but a promiscuous cell surface antigen following IFN stimulation. J. Immunol. **177:**3260–3265.
8. **Cadwell, K., and L. Coscoy.** 2005. Ubiquitination on nonlysine residues by a viral E3 ubiquitin ligase. Science **309:**127–130.
9. **Chang, L. J., V. Urlacher, T. Iwakuma, Y. Cui, and J. Zucali.** 1999. Efficacy and safety analyses of a recombinant human immunodeficiency virus type 1 derived vector system. Gene Ther. **6:**715–728.
10. **Coscoy, L.** 2007. Immune evasion by Kaposi's sarcoma-associated herpesvirus. Nat. Rev. Immunol. **7:**391–401.
11. **Coscoy, L., and D. Ganem.** 2000. Kaposi's sarcoma-associated herpesvirus encodes two proteins that block cell surface display of MHC class I chains by enhancing their endocytosis. Proc. Natl. Acad. Sci. USA **97:**8051–8056.
12. **Coscoy, L., D. J. Sanchez, and D. Ganem.** 2001. A novel class of herpesvirus-encoded membrane-bound E3 ubiquitin ligases regulates endocytosis of proteins involved in immune recognition. J. Cell Biol. **155:**1265–1273.
13. **Deveraux, Q., V. Ustrell, C. Pickart, and M. Rechsteiner.** 1994. A 26 S protease subunit that binds ubiquitin conjugates. J. Biol. Chem. **269:**7059–7061.
14. **Douglas, J., K. Viswanathan, M. N. McCarroll, J. Gustin, K. Früh, and A. Moses.** 2009. Vpu directs the degradation of the human immunodeficiency virus restriction factor BST-2/tetherin via a βTrCP-dependent mechanism. J. Virol. **83:**7931–7947.
15. **Duncan, L. M., S. Piper, R. B. Dodd, M. K. Saville, C. M. Sanderson, J. P. Luzio, and P. J. Lehner.** 2006. Lysine-63-linked ubiquitination is required for endolysosomal degradation of class I molecules. EMBO J. **25:**1635–1645.
16. **Früh, K., E. Bartee, K. Gouveia, and M. Mansouri.** 2002. Immune evasion by a novel family of viral PHD/LAP-finger proteins of gamma-2 herpesviruses and poxviruses. Virus Res. **88:**55–69.
17. **Fuld, S., C. Cunningham, K. Klucher, A. J. Davison, and D. J. Blackbourn.** 2006. Inhibition of interferon signaling by the Kaposi's sarcoma-associated herpesvirus full-length viral interferon regulatory factor 2 protein. J. Virol. **80:**3092–3097.
18. **Garrus, J. E., U. K. von Schwedler, O. W. Pornillos, S. G. Morham, K. H. Zavitz, H. E. Wang, D. A. Wettstein, K. M. Stray, M. Cote, R. L. Rich, D. G. Myszka, and W. I. Sundquist.** 2001. Tsg101 and the vacuolar protein sorting pathway are essential for HIV-1 budding. Cell **107:**55–65.
19. **Gottlinger, H. G.** 2008. HIV/AIDS: virus kept on a leash. Nature **451:**406–408.
20. **Grossmann, C., S. Podgrabinska, M. Skobe, and D. Ganem.** 2006. Activation of NF-kappaB by the latent vFLIP gene of Kaposi's sarcoma-associated herpesvirus is required for the spindle shape of virus-infected endothelial cells and contributes to their proinflammatory phenotype. J. Virol. **80:**7179–7185.
21. **Hicke, L., and R. Dunn.** 2003. Regulation of membrane protein transport by ubiquitin and ubiquitin-binding proteins. Annu. Rev. Cell Dev. Biol. **19:**141–172.
22. **Joo, C. H., Y. C. Shin, M. Gack, L. Wu, D. Levy, and J. U. Jung.** 2007. Inhibition of interferon regulatory factor 7 (IRF7)-mediated interferon signal transduction by the Kaposi's sarcoma-associated herpesvirus viral IRF homolog vIRF3. J. Virol. **81:**8282–8292.
23. **Jouvenet, N., S. J. Neil, M. Zhadina, T. Zang, Z. Kratovac, Y. Lee, M. McNatt, T. Hatziioannou, and P. D. Bieniasz.** 2009. Broad-spectrum inhibition of retroviral and filoviral particle release by tetherin. J. Virol. **83:**1837–1844.
24. **Krishnan, H. H., P. P. Naranatt, M. S. Smith, L. Zeng, C. Bloomer, and B. Chandran.** 2004. Concurrent expression of latent and a limited number of lytic genes with immune modulation and antiapoptotic function by Kaposi's sarcoma-associated herpesvirus early during infection of primary endothelial and fibroblast cells and subsequent decline of lytic gene expression. J. Virol. **78:**3601–3620.
25. **Kupzig, S., V. Korolchuk, R. Rollason, A. Sugden, A. Wilde, and G. Banting.** 2003. Bst-2/HM1.24 is a raft-associated apical membrane protein with an unusual topology. Traffic **4:**694–709.
26. **Lehner, P. J., S. Hoer, R. Dodd, and L. M. Duncan.** 2005. Downregulation of cell surface receptors by the K3 family of viral and cellular ubiquitin E3 ligases. Immunol. Rev. **207:**112–125.
27. **Li, Q., R. Means, S. Lang, and J. U. Jung.** 2006. Downregulation of interferon gamma receptor 1 by Kaposi's sarcoma-associated herpesvirus K3 and K5. J. Virol. **81:**2117–2127.
28. **Lorenzo, M. E., J. U. Jung, and H. L. Ploegh.** 2002. Kaposi's sarcoma-associated herpesvirus K3 utilizes the ubiquitin-proteasome system in routing class I major histocompatibility complexes to late endocytic compartments. J. Virol. **76:**5522–5531.
29. **Loureiro, J., and H. L. Ploegh.** 2006. Antigen presentation and the ubiquitin-proteasome system in host-pathogen interactions. Adv. Immunol. **92:**225–305.
30. **Mansouri, M., E. Bartee, K. Gouveia, B. T. Hovey Nerenberg, J. Barrett, L. Thomas, G. Thomas, G. McFadden, and K. Früh.** 2003. The PHD/LAP-domain protein M153R of myxomavirus is a ubiquitin ligase that induces the rapid internalization and lysosomal destruction of CD4. J. Virol. **77:**1427–1440.

31. **Mansouri, M., J. Douglas, P. P. Rose, K. Gouveia, G. Thomas, R. E. Means, A. V. Moses, and K. Früh.** 2006. Kaposi's sarcoma herpesvirus K5 eliminates CD31/PECAM from endothelial cells. Blood **108:**1932–1940.
32. **Mansouri, M., P. P. Rose, A. V. Moses, and K. Früh.** 2008. Remodeling of endothelial adherens junctions by Kaposi's sarcoma herpesvirus. J. Virol. **82:**9615–9628.
33. **Melikova, M. S., K. A. Kondratov, and E. S. Kornilova.** 2006. Two different stages of epidermal growth factor (EGF) receptor endocytosis are sensitive to free ubiquitin depletion produced by proteasome inhibitor MG132. Cell Biol. Int. **30:**31–43.
34. **Mettenleiter, T. C.** 2002. Herpesvirus assembly and egress. J. Virol. **76:**1537–1547.
35. **Mimnaugh, E. G., H. Y. Chen, J. R. Davie, J. E. Celis, and L. Neckers.** 1997. Rapid deubiquitination of nucleosomal histones in human tumor cells caused by proteasome inhibitors and stress response inducers: effects on replication, transcription, translation, and the cellular stress response. Biochemistry **36:**14418–14429.
36. **Miyagi, E., A. J. Andrew, S. Kao, and K. Strebel.** 2009. Vpu enhances HIV-1 virus release in the absence of Bst-2 cell surface down-modulation and intracellular depletion. Proc. Natl. Acad. Sci. USA **106:**2868–2873.
37. **Moses, A. V., K. N. Fish, R. Ruhl, P. P. Smith, J. G. Strussenberg, L. Zhu, B. Chandran, and J. A. Nelson.** 1999. Long-term infection and transformation of dermal microvascular endothelial cells by human herpesvirus 8. J. Virol. **73:**6892–6902.
38. **Mukhopadhyay, D., and H. Riezman.** 2007. Proteasome-independent functions of ubiquitin in endocytosis and signaling. Science **315:**201–205.
39. **Nakatsukasa, K., and J. L. Brodsky.** 2008. The recognition and retrotranslocation of misfolded proteins from the endoplasmic reticulum. Traffic **9:**861–870.
40. **Nathan, J. A., and P. J. Lehner.** 2009. The trafficking and regulation of membrane receptors by the RING-CH ubiquitin E3 ligases. Exp. Cell Res. **315:**1593–1600.
41. **Neil, S. J., T. Zang, and P. D. Bieniasz.** 2008. Tetherin inhibits retrovirus release and is antagonized by HIV-1 Vpu. Nature **451:**425–430.
42. **Offermann, M. K.** 2007. Kaposi sarcoma herpesvirus-encoded interferon regulator factors. Curr. Top. Microbiol. Immunol. **312:**185–209.
43. **Ohmura-Hoshino, M., E. Goto, Y. Matsuki, M. Aoki, M. Mito, M. Uematsu, H. Hotta, and S. Ishido.** 2006. A novel family of membrane-bound E3 ubiquitin ligases. J. Biochem. (Tokyo) **140:**147–154.
44. **Ohtomo, T., Y. Sugamata, Y. Ozaki, K. Ono, Y. Yoshimura, S. Kawai, Y. Koishihara, S. Ozaki, M. Kosaka, T. Hirano, and M. Tsuchiya.** 1999. Molecular cloning and characterization of a surface antigen preferentially overexpressed on multiple myeloma cells. Biochem. Biophys. Res. Commun. **258:**583–591.
45. **Pantanowitz, L., K. Früh, S. Marconi, A. V. Moses, and B. J. Dezube.** 2008. Pathology of rituximab-induced Kaposi sarcoma flare. BMC Clin. Pathol. **8:**7.
46. **Raggo, C., R. Ruhl, S. McAllister, H. Koon, B. J. Dezube, K. Früh, and A. V. Moses.** 2005. Novel cellular genes essential for transformation of endothelial cells by Kaposi's sarcoma-associated herpesvirus. Cancer Res. **65:**5084–5095.
47. **Sakakibara, S., C. A. Pise-Masison, J. N. Brady, and G. Tosato.** 2008. Gene regulation and functional alterations induced by Kaposi's sarcoma herpesvirus-encoded ORFK13/vFLIP in endothelial cells. J. Virol. **83:**2140–2153.
48. **Saksena, S., J. Sun, T. Chu, and S. D. Emr.** 2007. ESCRTing proteins in the endocytic pathway. Trends Biochem. Sci. **32:**561–573.
49. **Sanchez, D. J., D. Miranda, Jr., V. Arumugaswami, S. Hwang, A. E. Singer, A. Senaati, A. Shahangian, M. J. Song, R. Sun, and G. Cheng.** 2008. A repetitive region of gammaherpesvirus genomic DNA is a ligand for induction of type I interferon. J. Virol. **82:**2208–2217.
50. **Stevenson, P. G., J. S. May, X. G. Smith, S. Marques, H. Adler, U. H. Koszinowski, J. P. Simas, and S. Efstathiou.** 2002. K3-mediated evasion of CD8(+) T cells aids amplification of a latent gamma-herpesvirus. Nat. Immunol. **3:**733–740.
51. **Sun, R., S. F. Lin, L. Gradoville, Y. Yuan, F. Zhu, and G. Miller.** 1998. A viral gene that activates lytic cycle expression of Kaposi's sarcoma-associated herpesvirus. Proc. Natl. Acad. Sci. USA **95:**10866–10871.
52. **Thibodeau, J., M.-C. Bourgeois-Daigneault, G. Huppé, J. Tremblay, A. Aumont, M. Houde, E. Bartee, A. Brunet, M.-E. Gauvreau, A. de Gassart, E. Gatti, M. Baril, M. Cloutie, S. Bontron, K. Früh, D. Lamarre, and V. Steimle.** 2008. Interleukin-10-induced MARCH1 mediates intracellular sequestration of MHC class II in monocytes. Eur. J. Immunol. **38:**1225–1230.
53. **Van Damme, N., D. Goff, C. Katsura, R. L. Jorgenson, R. Mitchell, M. C. Johnson, E. B. Stephens, and J. Guatelli.** 2008. The interferon-induced protein BST-2 restricts HIV-1 release and is downregulated from the cell surface by the viral Vpu protein. Cell Host Microbe **3:**245–252.
54. **van Weert, A. W., K. W. Dunn, H. J. Gueze, F. R. Maxfield, and W. Stoorvogel.** 1995. Transport from late endosomes to lysosomes, but not sorting of integral membrane proteins in endosomes, depends on the vacuolar proton pump. J. Cell Biol. **130:**821–834.
55. **Vieira, J., and P. M. O'Hearn.** 2004. Use of the red fluorescent protein as a marker of Kaposi's sarcoma-associated herpesvirus lytic gene expression. Virology **325:**225–240.
56. **Wang, X., R. A. Herr, and T. Hansen.** 2008. Viral and cellular MARCH ubiquitin ligases and cancer. Semin. Cancer Biol. **18:**441–450.
57. **Zhu, F. X., X. Li, F. Zhou, S. J. Gao, and Y. Yuan.** 2006. Functional characterization of Kaposi's sarcoma-associated herpesvirus ORF45 by BAC-based mutagenesis. J. Virol. **80:**12187–12196.